

SYNTHESIS, CHARACTERIZATION AND BIOCOMPATIBILITY OF CHITOSAN FUNCTIONALIZED NANOCARRIER FOR CONTROLLED AND CURING OF CANCER CELLS

Sivalingam Lakshmanan

Department of Chemistry, BIHER, Bharath University, Chennai 600 073, India

E-mail:lachuchem666@gmail.com

Abstract

This study reports the in vitro cytotoxic effect of Curcumin (CR)-loaded chitosan (CS)-cross-linked polybutylene glycol (PBG) nanocarriers. The nanocarriers were prepared by ion gelation using barium chloride ($BaCl_2$), calcium oxalate ($Ca(COO)_2$), and sodium tripolyphosphate (TPP) as cross-linking agents. The influence of the cross-linking agent on the size and morphology of the CS-PBG nanocarriers was studied by dynamic light scattering (DLS) and scanning electron microscope (SEM). TPP assisted carriers was found higher amount CR encapsulation capacity compared with other two carriers. The drug releasing behavior was studied at pH 6.8 which was based on the bulk erosion principle of the carriers. CR loaded CS-PBG carriers were found to show excellent drug releasing kinetics and biocompatibility in in-vitro analysis.

Key words: Chitosan; Curcumin; cell uptake; in vitro

Introduction

Advances in nanotechnology for treatment of diseases have led to growth of the interdisciplinary field of nanomedicine. Nanotherapy is less harmful than conventional therapies, and is believed to improve the quality of treatment in terms of diagnosis, controlled drug delivery, and imaging, and to reduce the patient burden¹. The objective of nanotherapy is targeted drug delivery at the lowest possible dose^{2,3}. Many nanocarriers have been developed for drug delivery applications⁴. Currently, researchers are working to develop effective treatments for the early stages of cancer with low side effects⁵. One of the major drawbacks of chemotherapy is that it is difficult to deliver therapeutics directly to the site of solid tumors, sometimes leading to treatment failure; nanotherapy can overcome this problem⁶⁻⁸. Nanomedicines can interact with biomolecules or receptors on the cell surface and easily gain entry to cells. Several synthetic chemotherapeutic agents are available for the treatment of cancer, but most have major drawbacks, such as non-selective distribution of drugs, toxicity, and side effects. Recently, curcumin (CR), a functional food that is rich in natural polyphenols, has attracted the attention of researchers, as it shows a range of health advantages as well as chemotherapeutic effects for cancer treatment^{9,10}. CR has been proven to exhibit antioxidant, anti-inflammatory¹¹ anti-microbial, anti-carcinogenic, hepatoprotective, and nephroprotective activities^{12,13}. Moreover, it protects against blood clots and heart attack¹⁴.

CR is extracted from the herb *curcuma longa*¹⁵. CR known to be effective an anticancer agent and even high doses of curcumin have been proven safe for normal cells¹⁶. CR embeds profound into the membrane of the hydrogen bond anchored and bi-layer orientation of lipids in a way closely resembling cholesterol¹⁷; this property indicates that CR has high potential activity for treatment of lung cancer.

However, the delivery of CR is complicated by its poor solubility in aqueous media, low bioavailability, low biodegradability, rapid metabolism, low gastrointestinal absorption, poor circulation time, and easy degradability under physiological conditions¹⁸. Given these drawbacks, various biodegradable polymeric nanocomposites have been developed as carriers to enhance bioavailability and to prevent degradation or elimination in the circulatory system, allowing CR to be delivered near cancer tissues. Previously, a nano-formulation of CR with a synthetic polymer and liposomes was developed in the attempt to increase the solubility and degradability of hydrophobic CR drugs¹⁹. However, this formulation failed to achieve sufficient

bioavailability, controlled drug-release kinetics, or target site delivery. Biopolymers can overcome these problems, thus natural polymers like chitosan, carboxymethyl cellulose, polyethylene glycol, poly(lactic acid) (PLA), poly(lactide-co-glycolide) (PLGA), and polyethylene glycol-co-polylactide (PEG-b-PLA) can be used as drug carriers; they have the additional benefit of not provoking an immune reaction^{20,21}.

The present work aimed to achieve size-controlled synthesis of a nanocarrier (CS cross-linked PBG) using different anionic cross-linking agents, such as BaCl₂, Ca(COO)₂, and Na₅P₃O₁₀, which are mono-, di-, and tri-cross-linking agents, respectively. The CS amine group is protonated by the anionic charge of BaCl₂, Ca(COO)₂, and TPP, and the NH₃⁺ group is neutralized by PBG. The addition of PBG to the chitosan formulation increases hydrophilicity. The method of ionic gelation has more merits (simple, mild, less toxic, and suitable for scaling up³⁰) than other techniques, such as the sol-gel, emulsion, and spray-drying methods³¹. The ionic gelation method involves ion-induction of polymer bonds between polymeric molecules by varying the charge on the cross-linking ion; the influence of the ion was characterized by measuring particle size, encapsulation efficiency, zeta potential, optical microscopic analysis, functional changes, and surface morphology.

2. Experimental Section

2.1 Materials

Chitosan (CS), polybutylene glycol (PBG), barium chloride (BaCl₂), calcium oxalate (Ca(COO)₂), sodium tri poly-phosphate (TPP), acetone, and ethanol were obtained from sigma Aldrich, India. CR and ethanol were purchased from Sigma-Aldrich, India. Analytical grade chemicals were used.

2.2 Preparation of nanocarriers

Chitosan (200 mg) was dissolved in 50 mL of 0.1 N acetic acid. Barium chloride (0.1%) was prepared in 25 mL of double-distilled water. Nano CS was prepared according to a previously described procedure, with slight modifications³². A BaCl₂ solution was added dropwise to a CS solution with continuous stirring at 30°C. PBG (25 mL, 0.2%) in water was added dropwise to the CS/BaCl₂ solution. After 1 h, the solution was collected and centrifuged at 6000 rpm for 20 min. The nanocomposites (CS-PBG-A) were dried and characterized for functional group changes and surface modifications. The above protocol was followed for the synthesis of CS-PBG-B and CS-PBG-C using Ca(COO)₂ and TPP, respectively, to replace the BaCl₂.

2.3 Fabrication of CR-loaded polymeric nanocarriers

Encapsulation of CR on the polymeric nanocarriers was performed using the ionic gelation technique. For encapsulation, 25 mg of CR was dissolved in 25 mL of ethanol. The ethanol portion was poured onto the CS solution while the solution was continuously stirred. The BaCl₂ solution was added dropwise to the CS-CR solution, followed by continuous stirring at room temperature. Then the PBG solution was added and the above procedure was followed. Synthesis of CS-CR-PBG-B and CS-CR-PBG-B was performed using BaCl₂, and Ca(COO)₂ and TPP were used as the respective cross-linking agents.

2.4. Characterization of the nanocomposites

2.4.1. Zeta potential of blank and drug-loaded nanoparticles

For the measurement of surface charge and zeta potential values of the nanoparticles, 10 mg of nanoparticles was suspended in 10 mL deionized water by using a Beckman Coulter unit (in add xxx). The data shown are the average of three measurements.

2.4.2. FT-IR spectroscopy analysis

Functional changes with and without the CR nanocomposites (CS-PBG-A, CS-CR-PBG-A, CS-PBG-B, CS-CR-PBG-B, CS-PBG-C, and CS-CR-PBG-C) were observed with a Fourier transform infrared spectrometer (instrument details add)

2.4.3. SEM analyses

2.5. Evaluation of encapsulation efficiency

The nanoparticle suspensions were separated by centrifugation at 6000 rpm for 20 min and their drug encapsulation efficiency (EE) was evaluated by measuring the absorption of the supernatant liquid using a UV spectrophotometer (Systronics, India) at a λ_{max} value of 417 nm. The corresponding calibration curves were calculated by testing the supernatant from blank nanoparticles. All measurements were performed in triplicate, and the mean values are reported.

2.6. In vitro controlled release studies

The *in vitro* drug release rates of the carriers with various beads were measured under environmental conditions at 30°C as follows: 100 mg of dried beads was placed in 30 mL of pH 6.8 buffer solution, with constant stirring using a magnetic stirrer. At pre-determined time intervals, certain volumes were gathered from the release medium for the examination of cur utilizing a UV–Vis spectrophotometer at a wavelength of 417 nm¹². These studies were performed in triplicate for each sample and average values were considered for data analysis.

2.7. Biological characterization

2.7.1. Cell viability assay using MCF-7 cells

Inhibition of cellular growth of the MCF-7 breast cancer cell line was measured using the 3-(4,5-dimethylthiazol-2-yl)-2,5-diphenyl tetrazolium bromide (MTT) assay, as described previously³³. MCF-7 breast cancer cells (5×10^3) in Minimum Essential Medium (MEM) enhanced with 10% FBS, 1% penicillin/streptomycin, and 0.15% insulin were seeded in 96-well plates and incubated for 24 h at 37°C in a CO₂ incubator. After incubation, every well was supplemented with 150 µL of fresh medium containing various concentrations (10–100 µM) of CS-CR-PBG-I, CS-CR-PBG-II, CS-CR-PBG-III, pure CR, and CS-PBG-III nanocomposites. Cells were then incubated at 37°C in a 5% CO₂ incubator for 24 h. After incubation, the medium was aspirated from every well and the cells were washed with PBS. For cell suitability estimations, 100 µL of fresh medium (free of phenol red) and 10 µL of MTT reagent (5 mg/mL in PBS) was added to every well and incubated for 4 h to permit the development of formazan crystals. The medium was aspirated from the wells and supplemented with 50 µL of dimethyl sulfoxide (DMSO) and incubated at 37°C for an extra 10 min to soluble the formazan. The absorbance results were measured utilizing a microplate reader (Bio-Rad Model 680) at 570 nm to decide the relative viabilities. The results are exhibited as average ± standard deviation.

3. Results and Discussion

3.1. Characterization of nanoparticles

3.1.1. Nature of the nanocomposites

The pharmaceutical potential of CR has been limited by its lack of aqueous solubility; however, nano CR may be a clear formulation, with a hue derived from the original color of CR³⁵. We formulated different nanocarriers for CR using three cross-linking agents to enhance the potential activity of the combination. The nanocarriers were formed immediately due to complexing between the positively charged chitosan and the negatively charged anionic agents such as Cl⁻, (COO)₂²⁻, and TPP³⁻ ion³⁶. The smallest formulations were obtained using tri-anionic TPP as the cross-linking molecule. The color change of the samples is due the variation of particle

size, with mean values of 348, 287, and 126 nm for CS-CR-PBG-A, CS-CR-PBG-B, and CS-CR-PBG-C, respectively.

The color shows clear evidence for the formation of nano CR in solution. The color differences of the three CR-loaded nanocomposites are shown in Fig 1. The results for the zeta potential and poly disparity index values are listed in S. Table 1. The zeta potential significantly increased as the cross-linking anionic charge increased. The tri-anion TPP showed higher protonation of the NH_3^+ group on the CS molecule than the other two agents. The PDI values decreased from the mono-anion to tri-anion. The lower PDI value observed for CS-CR-PBG-C might correspond to higher protonation and stability during storage. The stability of nanoparticles in higher anionic agents is due to the steric repulsion of the TPP ions³⁷. Thus, the mono- to tri-anionic agents influence the size of the nanoparticles³⁸.

The stability of the loaded and unloaded nanocomposites was evaluated by measuring the zeta potential. The zeta potential values also indicated the surface charges of the particles. The zeta potential values of CS-CR-PBG-C showed greater stability than the other composites. The total repulsive forces between the particles may also improve the physical stability of multiphase systems³⁹.

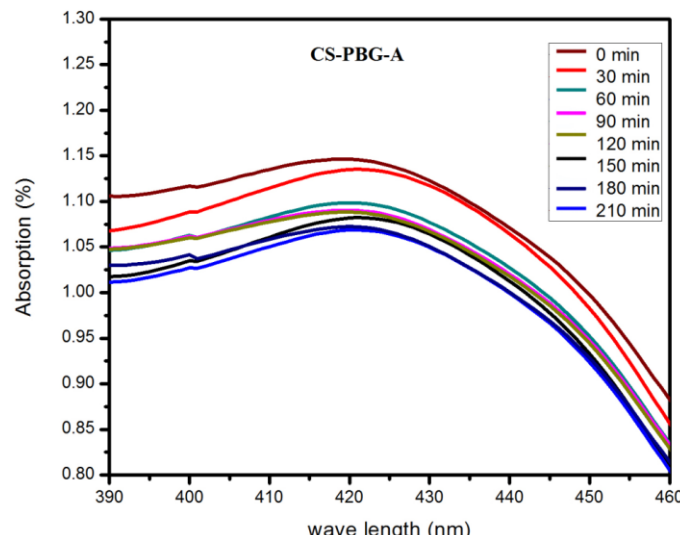


Figure 1. Color differences following the formation of nanoparticles (a) pure CR dissolved in ethanol, (b) CS-CR-PBG-A, (c) CS-CR-PBG-B, and (d) CS-CR-PBG-C.

3.1.2. FT-IR analysis

FT-IR analysis was performed to confirm nanocarrier formation and CR loading; the FT-IR spectra of unloaded and CR-loaded nanocomposites are shown in Fig 2. The characteristic amide bond bending vibration frequency peak was observed at 1642 cm^{-1} for CS-PBG-A, 1681 cm^{-1} for CS-PBG-B, and 1654 cm^{-1} for CS-PBG-C. The amide bond bending vibration peaks thus shifted from a lower region to a higher region; this is due to the interaction of the CS and PBG molecules in the composites. The ether starching vibration peak of PBG was observed at 1930 cm^{-1} in all CS-PBG carriers. No change was observed after the addition of CR to the carriers, confirming that no chemical reaction occurred between drug and carrier. The CS molecule C-N stretching vibration band was observed at 1389 , 1396 , and 1396 cm^{-1} for carrier samples A, B, and C, respectively, while the amide frequency changed from 1640 – 1650 cm^{-1} owing to variation in the cross-linking agents. Furthermore, a broad band was observed at 3400 – 3450 cm^{-1} in all spectra, which indicated the presence of the hydroxyl groups of the CS and PBG polymeric carriers. After CR loading, the hydroxyl group peak of all composites was observed at 3400 – 3450 cm^{-1} and changed from broad to sharp. This is due to the encapsulation of CR, because after the encapsulation of CR availability of intra molecular hydrogen bonding is decreased.

3.1.3. SEM and microscopic analysis

The SEM images of the resultant particles showed the particle size of CR-loaded and unloaded carrier formulated with mono, di, and tri anionic cross-linking agents gradually decreased. The surface morphology of the particles was smooth to spherical, as shown in Fig 4. The CS-PBG-A particles were irregular in structure and likely to be rod shaped, whereas the CS-PBG-B and CS-PBG-C particles were regularly spherical in shape. This suggests the influence of the anionic cross-linking agents during protonation of CS; CS cross-linked with PBG is more ordered than the other two systems.

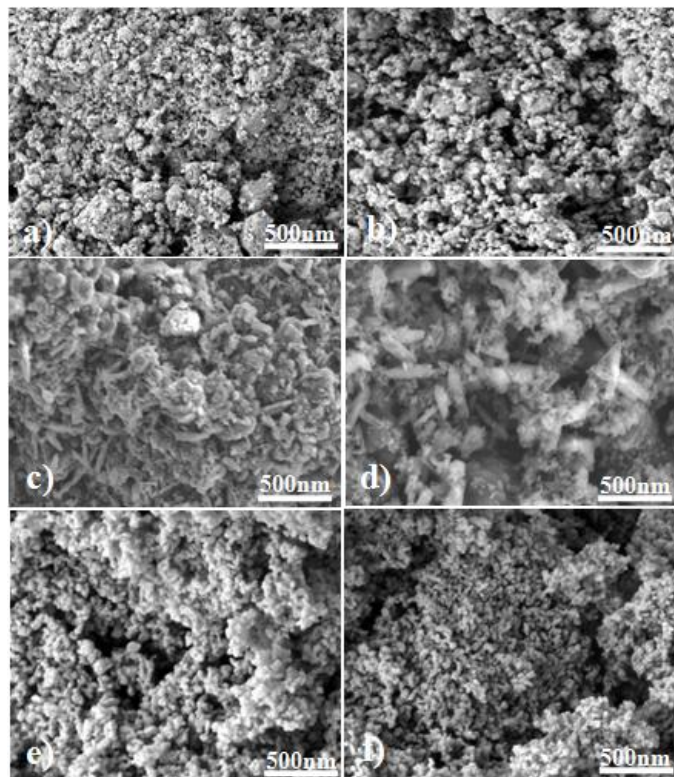


Figure 4. SEM images of CR-loaded and unloaded nanocomposites (A) CS-PBG-A, (B) CS-CR-PBG-A, (C) CS-PBG-B, (D) CS-CR-PBG-B, (E) CS-PBG-C, and (F) CS-CR-PBG-C.

3.2. Encapsulation and *in vitro* CR release

The encapsulation efficiency of CS-PBG-A, CS-PBG-B, and CS-PBG-C is illustrated in Fig. 6. Encapsulation of CR by all composites increased with time. Drug encapsulation is dependent on the encapsulation method and drug solubility. CR is hydrophobic, and the encapsulation of a hydrophobic drug is influenced by the method followed as well as the cross-linking agents used for reduction and stabilization of the carriers. CS-PBG-C showed faster encapsulation than the other nanocarriers. The initial concentration of CR also played an important role in the encapsulation efficiency. The TPP cross-linked CS-PBG carrier had higher encapsulation efficiency than the other two, because the particles were cleaved regularly without aggregation, so when CR enters the carrier, it is easily caught and bonded. The drug-release behavior of CS-PBG-C was studied at pH 6.8 using the dialysis membrane technique (S. Fig. 5). CR was gradually released from the carrier, and 25% CR release took more than 70 min, but 60% CR release was achieved within the subsequent 15 min. Because, the initial hydration of the carriers take more time, then it is easily diffused, creating voids. Another reason may be the number of positively charged amines present in chitosan preventing penetration of acidic media, thereby facilitating gradual release of CR from CS-PBG carriers⁴¹. After maximum composite swelling, the CR was easily released. The remaining CR was gradually released from the carriers during nearly 210 min. These results

are concordant with previously reported results for CR release from N-isopropyl acrylamide with N-vinyl-2-pyrrolidone (VP) and poly(ethylene glycol) monoacrylate polymeric nanoparticle systems³⁵.

3.3. Study of cell viability by MTT assay

Various concentrations (10 to 100 µg/mL) of CR-loaded CS-PBG-A, CS-PBG-B, CS-PBG-C, and unloaded CS-PBG-C were used to study effectiveness against MCF-7 breast cancer cells. All concentrations of unloaded composites tested against MCF-7 cells showed no toxic effects. The biodegradable polymers consistently showed cell adhesion 4- to 10-fold greater than empty wells²². Based on this observation, the carriers do not affect the cells. However, the CR-encapsulating CS-PBG-A, CS-PBG-B, and CS-PBG-C composites had a significant effect against MCF-7 breast cancer cells. Treatment with CS-CR-PBG-C showed higher cytotoxicity than the other composites. The IC₅₀ values of CS-CR-PBG-A, CS-CR-PBG-B, and CS-CR-PBG-C were 51.0, 55.4 and 38.7 µg/mL, respectively (Fig. 7). The results of this study suggests that the cytotoxicity of the three CR-loaded composites increased as CR encapsulation increased; because the CS-CR-PBG-C system contained a higher quantity of CR, it showed higher cytotoxicity than the other two. CS-CR-PBG-A, CS-CR-PBG-B, CS-CR-PBG-C, CS-PBG-C, and CR showed no cytotoxicity against normal cells (VERO); the results are shown in S. Fig. 9. Thus, the nanocarriers designed in this study had no effect on cells, and encapsulated CR showed cytotoxicity against cancer cells.

4. Conclusion

Nanotherapy technology was used to enhance the therapeutic properties of CR. Synthesis of a nano-carrier using a simple and cost-effective method via ion-gelation with various cross-linking agents was demonstrated. The size of the carriers was controlled by changing the cross-linking agents. The hydrophobic anticancer compound CR was successfully encapsulated in three different carriers. The ion-gelation process was optimized, using BaCl₂, Ca(COO)₂, and Na₅P₃O₁₀ for encapsulation of CR in the 300 -125 nm rod and spheres with smooth surface. Carriers formulated using TPP showed high encapsulation efficiency. *In vitro* drug release of CR from the carriers required nearly 3 h. *In vitro* cytotoxicity analysis showed that the nanotherapy composites arrested the growth of MCF-7 cells. The CS-PBG cross-linked nanocarrier formulated using TPP was found to show potential for use in delivering the natural anti-cancer drug CR for targeted nanotherapy.

References

1. O.C. Farokhzad, R. Langer. Impact of nanotechnology on drug delivery, ACS Nano. 3 (2009) 16–20, DOI: 10.1021/nn900002m.
2. N. Kamaly, Z. Xiao, P.M. Valencia, A.F. Radovic-Moreno, O.C. Farokhzad, Targeted polymeric therapeutic nanoparticles: design, development and clinical translation, Chem Soc Rev. 41(2012) 2971–3010, doi: 10.1039/c2cs15344k.
3. Y. Sun, Z. Sun, Transferrin-conjugated polymeric nanomedicine to enhance the anticancer efficacy of edelfosine in acute myeloid leukemia, Biomedicine & Pharmacotherapy. 83 (2016) 51-57, doi:10.1016/j.biopha.2016.05.046
4. M. Jeyaraj, R. Amarnath Praphakar, C. Rajendran, D. Ponnamma, K. Kumar Sadasivuni, M. A. Munusamy and M. Rajan, Surface functionalization of natural lignin isolated from *Aloe barbadensis Miller* biomass by atom transfer radical polymerization for enhanced anticancer efficacy, RSC Adv. 6 (2016) 51310–51319, DOI: 10.1039/C6RA01866A.
5. P.P.S. Vijay, T. Nandibewoor, Electroanalytical method for the determination of 5-fluorouracil using a reduced graphene oxide/chitosan modified sensor, RSC Adv 5 (2015) 34292-34301, DOI: 10.1039/C5RA04396D.

6. T. Helleday, E. Petermann, C. Lundin, B. Hodgson, R.A. Sharma, DNA repair pathways as targets for cancer therapy, *Nat Rev Cancer.* 8 (2008) 193–204, doi: 10.1038/nrc2342.
7. J. Liu, L. Xu, C. Liu, D. Zhang, S .Wang, Z .Deng, W. Lou, H. Xu, Q .Bai, J . Ma, Preparation and characterization of cationic CRcumin nanoparticles for improvement of cellular uptake, *Carbohydr Polym.* 90 (2012)16–22, doi:10.1016/j.carbpol.2012.04.036
8. T.P. Sari, B. Mann, R. Kumar, R.R.B. Singh, R. Sharma, M. Bhardwaja, S. Athira. Preparation and characterization of nanoemulsion encapsulating CRcumin, *Food Hydrocolloids.* 43 (2015) 540–554, doi:10.1016/j.foodhyd.2014.07.011.
9. L. Liu, X. Qi, Z. Zhong, E. Zhang, Nanomedicine-based combination of gambogic acid and retinoic acid chlorochalcone for enhanced anticancer efficacy in osteosarcoma, *Biomedicine & Pharmacotherapy.* 83 (2016) 79-84, doi:10.1016/j.biopha.2016.06.001
10. Ozge Berrak, Yunus Akkoç, Elif Damla Arısan, Ajda Çoker-Gürkan, Pınar Obakan-Yerlikaya, Narçin Palavan-Unsal, The inhibition of PI3K and NFκB promoted CRcumin-induced cell cycle arrest at G2/M via altering polyamine metabolism in Bcl-2 overexpressing MCF-7 breast cancer cells, *Biomedicine & Pharmacotherapy.* 77 (2016) 150-160.
11. N. Kasoju, U. Bora, Fabrication and characterization of CRcumin-releasing silk fibroin scaffold, *J. Biomed. Mater. Res.* 100B (2012) 1854–1866. doi: 10.1002/jbm.b.32753, doi: 10.1002/jbm.b.32753.
12. H. Geng, R. Li, Y. Su, J. Xiao, M. Pan, X. Cai, X. Ji, CRcumin protects cardiac myocyte against hypoxia-induced apoptosis through upregulating miR-7a/b expression, *Biomedicine & Pharmacotherapy.* 81 (2016) 258-264. doi: 10.1016/j.biopha.2016.04.020.
13. M.D. Toborek, S. Kaiser, Endothelial cell functions: relationship to atherogenesis, *Basic Res Cardiol.* 94 (1999) 295–314.
14. H.S. Koop, R.A. de Freitas, de Souza MM, Savi Jr. R, Silveira JLM. Topical CRcumin-loaded hydrogels obtained using galactomannan from *Schizolobium parahybae* and xanthan. *Carbohydr Polym* 2015;116: 229–236.
15. P. Anand, A.B. Kunnumakkara, R.A. Newman, B.B. Aggarwal. Bioavailability of CRcumin: problems and promises, *Mol Pharmaceutics.* 4 (2007) 807–818, DOI: 10.1021/mp700113r
16. J. Barry, M. Fritz, J.R. Brender, P.E.S. Smith, D-K. Lee, A. Ramamoorthy, Determining the effects of lipophilic drugs on membrane structure by solid-state NMR spectroscopy: The case of the antioxidant CRcumin, *J Am Chem Soc.* 131 (2009) 4490–4498, DOI: 10.1021/ja809217u.
17. H.u. Liandong, S.Pang, Q. Hu, D. Gu, D. Kong, X. Xiong, J. Su, Enhanced antitumor efficacy of folate targeted nanoparticles co-loaded with docetaxel and CRcumin, *Biomedicine & Pharmacotherapy.* 75 (2015) 26-32, doi: 10.1016/j.biopha.2015.08.036.
18. H. Yu, Q. Huang, Improving the oral bioavailability of CRcumin using novel organogel-based nanoemulsions. *J Agric Food Chem.* 60 (2012) 5373–5379, DOI: 10.1021/jf300609p.
19. G-F. Luo, X-D. Xu, J. Zhang, J. Yang, Y-H. Gong, Q. Lei, H-Z. Jia, C. Li, R-X. Zhuo, X-Z. Zhang. Encapsulation of an adamantane-doxorubicin prodrug in phresponsive polysaccharide capsules for controlled release, *ACS Appl Mater Interfaces.* 4 (2012) 5317–5324, DOI: 10.1021/am301258a.
20. G. Prabha, V. Raj, Formation and characterization of β-cyclodextrin (β-CD) – polyethyleneglycol (PEG) – polyethyleneimine (PEI) coated Fe₃O₄ nanoparticles for loading and releasing 5-Fluorouracil drug, *Biomedicine & Pharmacotherapy.* 80 (2016) 173-182, doi: 10.1016/j.biopha.2016.03.015.

21. S. Theapsak, A. Watthanaphanit, R. Rujiravanit, Preparation of chitosan-coated polyethylene packaging films by DBD plasma treatment, *ACS Appl Mater Interfaces*. 4 (2012) 2474–2482, doi: 10.1021/am300168a.
22. V. Alinejad, M.H. Somi, B. Baradaran, P. Akbarzadeh, F. Atyabi, H. Kazerooni, H. S. Kafil, L. A. Maleki, H. S. Mansouri, M. Yousefi, Co-delivery of IL17RB siRNA and doxorubicin by chitosan-based nanoparticles for enhanced anticancer efficacy in breast cancer cells, *Biomedicine & Pharmacotherapy*, 83 (2016) 229-240, doi:10.1016/j.biopha.2016.06.037
23. K. YG, S.S. Shin, U.S. Choi, Y.S. Park, J.W. Woo. Gelation of chitin and chitosan dispersed suspensions under electric field: effect of degree of deacetylation, *ACS Appl Mater Interfaces*. 3 (2011) 1289–1298, doi: 10.1021/am200091r.
24. M. Rajan, V. Raj. Potential drug delivery applications of chitosan based nanomaterials, *IRECHE*. 5 (2013) 145–155.
25. M. Rajan, V. Raj. Chitosan-polylacticacid-polyethylene glycol-gelatin nanoparticles: A novel biosystem for controlled drug delivery, *Carbohydr Polym*. 98 (2013) 951– 958, doi: 10.1016/j.carbpol.2013.05.025.
26. A. Singuin, P. Hubert, E. Dellacherie, Intermolecular associations in hydrophobically modified derivatives of propyleneglycol alginate, *Polymer*. 35(1994) 3557–3560, doi:10.1016/0032-3861(94)90923-7
27. S. Fusco, H-W. Huang, K.E. Peyer, C. Peters, M. Haberli, A. Ulbers, A. Spyrogianni, E. Pellicer, J. Sort, S.E. Pratsinis, B.J. Nelson, M.S. Sakar, S. Pane, Shape-switching microrobots for medical applications: The influence of shape in drug delivery and locomotion, *ACS Appl Mater Interfaces*. 7 (2015) 6803–6811,
28. R. Kunii, H. Onishi, Y. Machida. Preparation and antitumor characteristics of PLA/(PEG-PBG-PEG) nanoparticles loaded with camptothecin, *Eur J Pharm Biopharm*. 67 (2007) 9–17, doi: 10.1016/j.ejpb.2007.01.012
29. N. Arya, S. Chakraborty, N. Dube, D.S. Katti. Electrospraying: A facile technique for synthesis of chitosan-based micro/nanospheres for drug delivery applications, *J. Biomed. Mater. Res.* 88B (2009)17–31, doi: 10.1002/jbm.b.31085
30. C-S. Yang, H-C. Wu, J-S. Sun, H-M. Hsiao, T-W. Wang, Thermo-induced shape-memory PEG-PCL copolymer as a dual drug-eluting biodegradable stent, *ACS Appl Mater Interfaces*. 5 (2013) 10985–10994, doi: 10.1021/acsami.5b00181
31. P. Calvo, C. Remunan-Lopez, J.L. Vila-Jato, M.J. Alonso. Novel hydrophilic chitosan-polyethylene oxide nanoparticles as protein carriers, *J Appl Polym Sci*. 63 (1997) 125–132,
32. C .Krishnaraj, P. Muthukumaran, R. Ramachandran, M.D. Balakumaran, P.T. Kalaichelvan. *Acalypha indica Linn*: Biogenic synthesis of silver and gold nanoparticles and their cytotoxic effects against MDA-MB-231, human breast cancer cells, *Biotechnol Rep.* 4 (2014) 42–49, doi:10.1016/j.btre.2014.08.002.
33. G. Xi, X. Hu, B. Wu, H. Jiang, C.Y. Young, Y. Pang, H .Yuan, Autophagy inhibition promotes paclitaxel-induced apoptosis in cancer cells, *Cancer Lett.* 307 (2011) 141–148-148, doi: 10.1016/j.canlet.2011.03.026.
34. A. Wang, F. Muhammad, W. Qi, N. Wang, L. Chen, G. Zhu, Acid-induced release of CRcumin from barium containing nanotheranostic excipient, *ACS Appl Mater Interfaces*. 6 (2014) 14377–14383, doi: 10.1021/am503655z.

35. H-S. Lee, M.Q. Yee, Y.Y. Eckmann, N.J. Hickok, D.M. Eckmann, R.J. Composto, Reversible swelling of chitosan and quaternary ammonium modified chitosan brush layers: Effect of pH and counter anion size and functionality, *J Mater Chem*. 22 (2012) 19605–19616, doi: 10.1039/C2JM34316A.
36. U. Klinkesorn, P. Sophanodora, P. Chinachoti, D.J. McClements, E. Decker. Stability of spray-dried tuna oil emulsions encapsulated with two-layered interfacial membranes, *J Agric Food Chem.* 53 (2005) 8365–8371, doi: 10.1021/jf050761r.
37. Y. Yang, S. Wang, Y. Wang, X. Wang, Q. Wang, M. Chen. Advances in self-assembled chitosan nanomaterials for drug delivery, *Biotechnol Adv.* 2014;32:1301–1316, doi:10.1016/j.biotechadv.2014.07.007.
38. M. Muller, Miscibility behavior and single chain properties in polymer blends: a bond fluctuation model study, *Theory Simul.* 8 (1999) 343-374, DOI: 10.1002/(SICI)1521-3919(19990701)8:4<343::AID-MATS343>3.0.CO;2-F.
39. N. Sanoj Rejinald, M. Muthunarayanan, N. Deepa, K.P. Chennazhi, S.V. Nair, R. Jayakumar, CRcumin-loaded biocompatible thermoresponsive polymeric nanoparticles for cancer drug delivery, *Int J Biol Macromol.* 47 (2010) 37–43, doi: 10.1016/j.jcis.2011.04.006.
40. P. Mukhopadhyay, K. Sarkar, S. Bhattacharya, R. Mishra, P.P. Kundu. Efficient oral insulin delivery by dendronized chitosan: in vitro and in vivo studies, *RSC Adv.* 4 (2014) 43890–43902, doi: 10.1039/C4RA07511K.
41. J.J . Pillai, A.K.T. Thulasidasan, R.J. Anto, D.N. Chithralekha, A. Narayanan, G.S.V Kumar, Folic acid conjugated cross-linked acrylic polymer (FA-CLAP) hydrogel for site specific delivery of hydrophobic drugs to cancer cells, *J Nano Biotechnology.* 12 (2014) 12-25, doi: 10.1186/1477-3155-12-25.
42. K. Lekha Nair, S. Jagadeeshan, A. Nair, G.S. Vinod Kumar, Biological evaluation of 5-fluorouracil nanoparticles for cancer chemotherapy and its dependence on the carrier, PLGA, *Int J Nanomedicine.* 6 (2011) 1685–1697, doi: 10.2147/IJN.S20165.
43. S-X, Cui, X-J, Qu, Y-Y, Xie, L ,Zhou, M, Nakata, M, Makuuchi, W, Tang, CRcumin inhibits telomerase activity in human cancer cell lines, *Int J Mol Med.* 18 (2006) 227–231.
44. J .Shao, D .Zheng, Z. Jiang, H. Xu, Y. Hu, X. Li, X. Lu, CRcumin delivery by methoxy polyethylene glycol–poly (caprolactone) nanoparticles inhibits the growth of C6 glioma cells, *Acta Biochim Biophys Sin.* 43 (2011) 267-74, doi: 10.1093/abbs/gmr011.
45. A. Mathew, T. Fukuda, Y .Nagaoka, T. Hasumura, H. Morimoto, Y. Yoshida, T. Maekawa, K .Venugopal, D.S. Kumar. CRcumin loaded-PLGA nanoparticles conjugated with Tet-1 peptide for potential use in Alzheimer's disease, *PLoS One.* 7 (2012) e32616, doi: 10.1371/journal.pone.0032616.